CATION-CHLORIDE CO-TRANSPORTER 1 (CCC1) Mediates Plant Resistance against *Pseudomonas syringae*[1]

Baoda Han,[a,2] Yunhe Jiang,[a,2] Guoxin Cui,[b] Jianing Mi,[a] M. Rob G. Roelfsema,[c] Grégory Mouille,[d] Julien Sechet,[d] Salim Al-Babili,[a] Manuel Aranda,[b] and Heribert Hirt[a,e,f,3,4]

[a]King Abdullah University of Science and Technology (KAUST), DARWIN21, Biological and Environmental Science & Engineering Division (BESE), Thuwal 23955-6900, Saudi Arabia

[b]King Abdullah University of Science and Technology (KAUST), Red Sea Research Center (RSRC), Biological and Environmental Science & Engineering Division (BESE), Thuwal, 23955-6900, Saudi Arabia

[c]Department of Molecular Plant Physiology and Biophysics, University of Würzburg, D-97082 Würzburg, Germany

[d]Institut Jean-Pierre Bourgin, INRA, AgroParisTech, CNRS, Université Paris-Saclay, 78000 Versailles, France

[e]Max Perutz Laboratories, University of Vienna, 1030 Vienna, Austria

[f]Institute of Plant Sciences Paris-Saclay IPS2, CNRS, INRA, Université Paris-Sud, Université Evry, Université Paris-Saclay, Bâtiment 630, 91405 Orsay, France

ORCID IDs: 0000-0002-7599-1422 (Y.J.); 0000-0003-4951-1883 (G.C.); 0000-0001-7846-9472 (J.M.); 0000-0002-4076-4246 (M.R.G.R.); 0000-0002-5493-754X (G.M.); 0000-0001-8398-4743 (J.S.); 0000-0003-4823-2882 (S.A.-B.); 0000-0001-6673-016X (M.A.); 0000-0003-3119-9633 (H.H.).

Plasma membrane (PM) depolarization functions as an initial step in plant defense signaling pathways. However, only a few ion channels/transporters have been characterized in the context of plant immunity. Here, we show that the Arabidopsis (*Arabidopsis thaliana*) $Na^+:K^+:2Cl^-$ (NKCC) cotransporter CCC1 has a dual function in plant immunity. CCC1 functions independently of PM depolarization and negatively regulates pathogen-associated molecular pattern-triggered immunity. However, CCC1 positively regulates plant basal and effector-triggered resistance to *Pseudomonas syringae* pv. *tomato* (*Pst*) DC3000. In line with the compromised immunity to *Pst* DC3000, *ccc1* mutants show reduced expression of genes encoding enzymes involved in the biosynthesis of antimicrobial peptides, camalexin, and 4-OH-ICN, as well as pathogenesis-related proteins. Moreover, genes involved in cell wall and cuticle biosynthesis are constitutively down-regulated in *ccc1* mutants, and the cell walls of these mutants exhibit major changes in monosaccharide composition. The role of CCC1 ion transporter activity in the regulation of plant immunity is corroborated by experiments using the specific NKCC inhibitor bumetanide. These results reveal a function for ion transporters in immunity-related cell wall fortification and antimicrobial biosynthesis.

Under natural conditions, plants are invariably challenged by harmful pathogens. However, plants possess several lines of defense mechanisms to protect themselves from disease (Hammond-Kosack and Jones, 1996; Hentschel, 2013). First, plants have unique cuticle and cell wall structural barriers, and they secrete antimicrobial peptides and chemical compounds to deter microbial invaders (Lamb et al., 1989; Hammond-Kosack and Jones, 1996; Hématy et al., 2009; Ahuja et al., 2012; Bacete et al., 2017). After escaping from this first line of plant defense, pathogens might reach the cell membrane, where a second layer of the plant immune system can be triggered (Jones and Dangl, 2006; Dodds and Rathjen, 2010). Here, plant cell-surface pattern recognition receptors detect pathogen-associated molecular patterns (PAMPs) to initiate PAMP-triggered immunity (PTI; Schwessinger and Zipfel, 2008; Bigeard et al., 2015). PTI is generally believed to be sufficient to halt nonpathogenic microbial growth (Xin and He, 2013). However, successful pathogens can breach PTI by deploying effectors to dampen PTI responses (Block and Alfano, 2011; Macho and

Zipfel, 2015). To counter effector-induced suppression of PTI, a large family of polymorphic nucleotide-binding/Leu-rich-repeat receptors can directly or indirectly detect the presence of specific effectors. Recognition of effectors triggers a third robust layer of resistance responses called effector-triggered immunity (ETI; Dou and Zhou, 2012; Feng and Zhou, 2012; Cui et al., 2015; Tang et al., 2017), which is essential to stop virulent pathogens from causing disease in certain plant genotypes (Lacombe et al., 2010; Xin and He, 2013).

Twenty years ago, it was shown that in cultured parsley cells, perception of PAMPs or effectors results in ion fluxes across the plasma membrane (PM) as one of the earliest defense responses (Jabs et al., 1997). Importantly, blocking ion fluxes by ion channel inhibitors prevented defense reactions, suggesting an important role of ion channels or transporters in plant defense against pathogens (Jabs et al., 1997). Thereafter, a large number of studies has been conducted on the molecular identity and function of ion channels/transporters in plant immunity. In mesophyll cells of Arabidopsis (*Arabidopsis thaliana*), Jeworutzki and colleagues described flg22- and elf18-induced PM depolarization functions as an initial step in the early signaling pathway of defense response (Jeworutzki et al., 2010). CYCLIC NUCLEOTIDE-GATED CHANNEL 2 (CNGC2) regulates Ca^{2+} influx, which activates calcium-dependent protein kinases. These calcium-dependent protein kinases regulate downstream PTI responses, linking cytosolic Ca^{2+} elevation to downstream defense reactions (Clough et al., 2000; Jurkowski et al., 2004; Ali et al., 2007; Boudsocq et al., 2010; Qi et al., 2010). Ca^{2+} signals also regulate the biosynthesis of salicylic acid (SA) by Calmodulin binding

transcription factor CBP60g (Wang et al., 2009). Anion channels are also required for defense responses, especially for PTI, as inhibition of rapid-type anion channels suppresses flg22-induced reactive oxygen species (ROS) production in Arabidopsis suspension cells (Colcombet et al., 2009). Arabidopsis guard cell SLOW ANION CHANNEL-ASSOCIATED 1 (SLAC1) is necessary to initiate stomatal closure upon pathogen treatment (Vahisalu et al., 2008; Koers et al., 2011; Montillet et al., 2013; Guzel Deger et al., 2015). Guo and colleagues reported that CHLORIDE CHANNEL D (CLC-D), which has both channel and transporter activities, is a negative regulator of PTI in Arabidopsis, demonstrating the importance of chloride channels in plant immunity (Guo et al., 2014). However, when compared with the extensive knowledge on Ca^{2+} signaling, the role and mechanistic basis of anions in plant immunity has been poorly characterized.

In animals, CCC family members mediate movement of Cl^- coupled with that of K^+ and/or Na^+ cations across the PMs (Hübner and Rust, 2006). There is only one *CCC* gene in Arabidopsis, referred to here as *CCC1*. Arabidopsis *CCC1* encodes a plant homolog of the animal $Na^+:K^+:2Cl^-$ cotransporter (NKCC), which was localized to the Golgi and trans-Golgi network (Henderson et al., 2015). Here, we investigated the role of CCC1 in the antibacterial defense response of Arabidopsis to three *Pseudomonas syringae* pv. *tomato* (*Pst*) DC3000 strains. *Pst* DC3000 carries about 30 effectors (Cunnac et al., 2011), which are delivered into plants via the type III secretion system (T3SS) and suppress plant defenses (Ishiga et al., 2011; Zhang et al., 2012; Johansson et al., 2015). *Pst* DC3000 *avrRpm1*, however, carries the *avrRpm1* gene that is recognized by
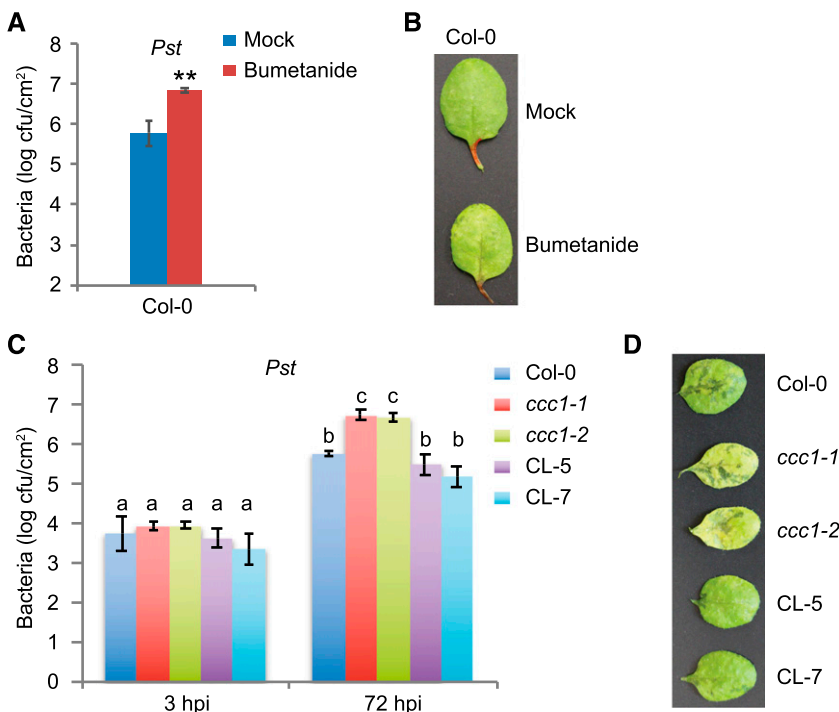

Figure 1. CCC1 is critical for resistance to virulent hemibiotrophic bacteria *Pst* DC3000. A, Growth of *Pst* DC3000 in wild-type plants treated with ethanol (mock) or bumetanide (100 nM) at 72 hpi. Four-week-old wild-type plants were inoculated by syringe-infiltration with *Pst* DC3000 suspension in 10 mM $MgSO_4$ at a density of 1×10^5 cfu/mL concomitantly with application of ethanol or bumetanide. Bacterial growth was quantified at 72 hpi. The data represent the mean ± SE, n = 8, P value < 0.01. B, Disease symptoms of wild type treated with ethanol or bumetanide at 72 hpi. C, Bacterial growth of *Pst* DC3000 in Col-0, *ccc1-1*, *ccc1-2*, CL-5, and CL-7 at 3 and 72 hpi. Four-week-old wild-type, *ccc1-1*, *ccc1-2*, CL-5, and CL-7 plants were spray-inoculated with bacterial suspensions in 10 mM $MgSO_4$ at a density of 1×10^8 cfu/mL. Bacterial growth was quantified at 3 and 72 hpi. The data represent the mean ± SE of eight biological replicates. Different letters denote statistically significant differences (P < 0.05, two-tailed t test) compared with wild-type plants at 3 hpi. D, Disease symptoms of the genotype mentioned in (C) at 96 hpi. All experiments were repeated at least two times with similar results.
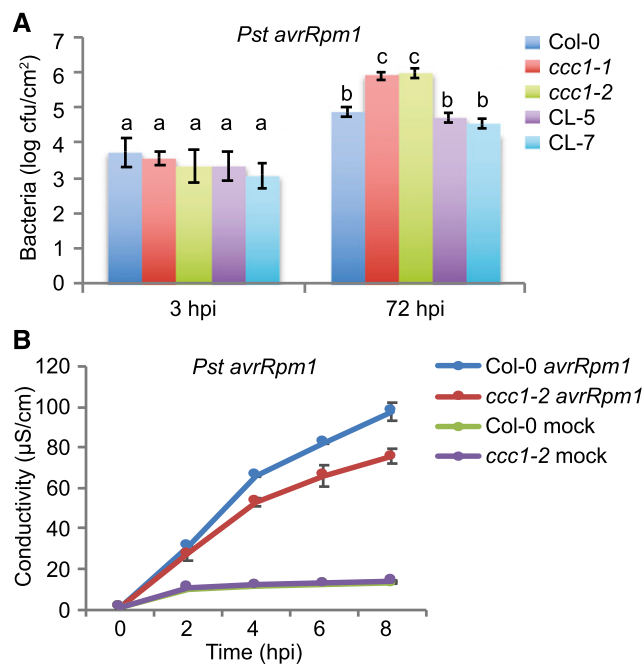
Figure 2. *ccc1* mutants showed reduced levels of ETI against *Pst* DC3000 *avrRpm1*. A, Bacterial growth of avirulent *Pst* DC3000 carrying the *avrRpm1* gene in Col-0, *ccc1-1*, *ccc1-2*, CL-5, and CL-7 at 3 and 72 hpi. Four-week-old Col-0, *ccc1-1*, *ccc1-2*, CL-5, and CL-7 plants were spray-inoculated with bacterial suspensions in 10 mM MgSO₄ at a density of 1×10^8 cfu/mL. Bacterial growth was quantified at 3 and 72 hpi. The data represent the mean ± SE of eight biological replicates. Different letters denote statistically significant differences ($P < 0.05$, two-tailed t test) compared with wild-type plants at 3 hpi. B, Ion leakage from leaf discs of wild-type and *ccc1-2* plants upon water or *Pst* DC3000 *avrRpm1* (OD_{600} = 0.1) treatment. Water and *Pst* DC3000 *avrRpm1* were infiltrated into leaves of wild type and *ccc1-2*, and ion leakage from leaf discs of wild type and *ccc1-2* was measured at the indicated time points. Error bars indicate SEs of two biological replicates. All experiments were repeated at least two times with similar results.

Arabidopsis RPM1 thereby rapidly inducing ETI responses that are mostly accompanied by a hypersensitive response at the infection sites (Xin and He, 2013). The third strain is *Pst* DC3000 *hrcC⁻*, in which the effectors cannot be delivered into the plant cell as the T3SS is defective. Hence, *Pst* DC3000 *hrcC⁻* only induces PTI and allows only very low proliferation of the *Pst* DC3000 *hrcC⁻* strain in plants (Jin and He, 2001).

We report here that CCC1 is not necessary for PM depolarization. However, CCC1 regulates both PTI and basal plant resistance to *Pst* DC3000. Surprisingly, although *ccc1* mutant plants are compromised in defense against virulent and avirulent *Pseudomonas syringae* pathogens, they show increased PTI responses and flg22-induced resistance to *Pst* DC3000. To elucidate the molecular mechanism of CCC1-mediated resistance, we performed global transcriptomic analysis of wild-type plants and *ccc1* mutants. Genes involved in the biosynthesis of antimicrobial peptides, defense chemical compounds, and *PR* proteins are repressed in

ccc1 mutants. Altered gene expression for cell wall functions in *ccc1* mutants corroborated changes in the composition of cell wall monosaccharides. Experiments using the NKCC-specific inhibitor bumetanide corroborate our findings, suggesting that ion channels play an important role in pathogen-related cell wall fortification and the synthesis of various antimicrobial compounds.

RESULTS

CCC1 Is Critical for Resistance to Virulent Hemibiotrophic Bacteria *Pst* DC3000

CCC1 was shown to encode the Arabidopsis homolog of the animal NKCC cotransporter, which is sensitive to the NKCC-specific inhibitor bumetanide (Colmenero-Flores et al., 2007). To investigate whether NKCC activity is required for antibacterial defense in Arabidopsis, 4-week-old wild-type plants were syringe-infiltrated with *Pst* DC3000 concomitantly with the application of ethanol (mock) or bumetanide. Bacterial growth was quantified at 72 h post inoculation (hpi). As shown in Figure 1A, bumetanide-treated plants showed considerably higher proliferation levels of *Pst* Dc3000 when compared with wild-type plants upon ethanol treatment. The higher bacterial titer in bumetanide-treated plants was associated with more severe chlorosis and necrosis formation (Fig. 1B), supporting that NKCC activity is involved in basal plant immunity.

To further confirm the role of CCC1 in antibacterial immunity, we assessed two independent *CCC1* transfer DNA (T-DNA) insertion lines, SALK-048175 (*ccc1-1*) and SALK-145300 (*ccc1-2*), which have T-DNA insertions in the first exon and first intron, respectively (Supplemental Fig. S1A). The mutant lines showed a stunted growth phenotype with a smaller rosette diameter compared with wild-type plants (Colmenero-Flores et al., 2007; Henderson et al., 2015; Supplemental Fig. S1B). Results from reverse transcription-quantitative PCR (RT-qPCR) confirmed that *ccc1-1* and *ccc1-2* are knockout mutants and have no detectable *CCC1* transcripts (Supplemental Fig. S1C). We spray-inoculated wild-type and *ccc1* mutant plants with *Pst* DC3000 and counted viable bacteria at 3 and 72 hpi. As shown in Figure 1C, bacterial growth in *ccc1* mutant plants was similar to wild type at 3 hpi, indicating that stomatal immunity is not affected in *ccc1* mutants (Fig. 1C). However, at 72 hpi, *ccc1* mutant plants showed significantly higher colony forming units (cfu) than wild-type plants (Fig. 1C). To ascertain that mutations in the *CCC1* gene are responsible for the observed susceptibility phenotype to *Pst* DC3000, *ccc1-2* was complemented with CCC1-GFP under the control of the ubiquitin promoter. Two representative complementation lines, CL-5 and CL-7, exhibited restored resistance to *Pst* DC3000 infection (Fig. 1C) and rescued the stunted growth phenotype of the *ccc1-2* mutant to the wild-type levels (Supplemental Fig. S1B). The CL-5 and CL-7 complementation lines also reverted the pathogen-induced necrosis phenotype observed in *ccc1* mutants
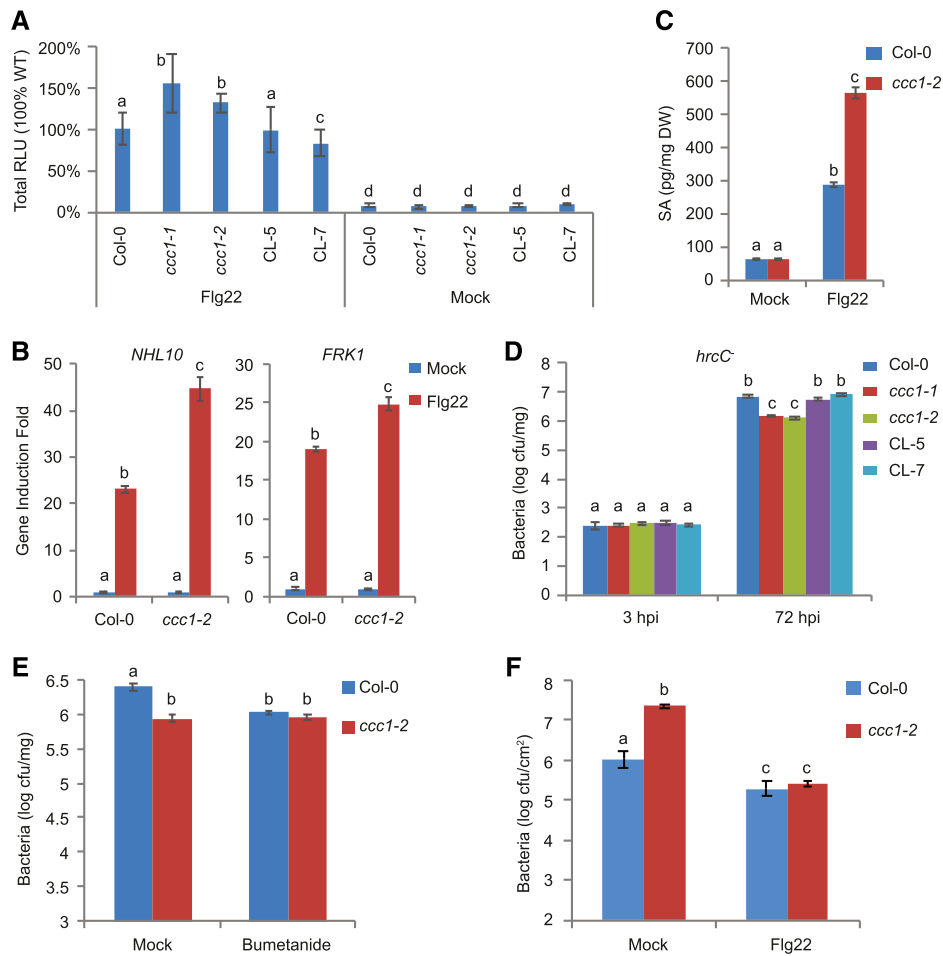
Figure 3. CCC1 suppresses PTI responses, disease resistance to *Pst* DC3000 *hrcC⁻*, and flg22-induced resistance to *Pst* DC3000. A, Flg22-induced early ROS bursts in Col-0, *ccc1-1*, *ccc1-2*, CL-5, and CL-7 were measured using a luminol-based assay (relative light units, RLU). Total ROS production is shown and refers to Col-0 treated with flg22 as 100%. Leaf discs from 4-week-old plants were treated with 1 μM flg22 for 40 min. $n = 9$. B, Induction of two PTI marker genes *NHL10* and *FRK1* after 1 μM flg22 treatment for 1 h in wild-type and *ccc1-2* plants; $n = 3$. C, Free SA accumulation was measured 24 h after treatment with WATER or 1 μM flg22 in 2-week-old Col-0 and *ccc1-2* seedlings; $n = 3$. D, Bacterial growth of nonpathogenic strain *Pst* DC3000 *hrcC⁻* in Col-0, *ccc1-1*, *ccc1-2*, CL-5, and CL-7. Two-week-old Col-0, *ccc1-1*, *ccc1-2*, CL-5, and CL-7 plants were flooded with bacterial suspensions in 10 mM MgSO$_4$ at a density of 1×10^7 cfu/mL, and bacterial growth was quantified at 3 and 72 hpi $n = 8$. E, Growth of *Pst* DC3000 *hrcC⁻* in wild-type and *ccc1-2* seedlings with ethanol (mock) or bumetanide (100 nM) treatment at 72 hpi. Two-week-old wild-type and *ccc1-2* seedlings grown on half-strength MS plate with ethanol or 100 nM bumetanide were flooded with *Pst* DC3000 suspension in 10 mM MgSO$_4$ at a density of 1×10^7 cfu/mL. Bacterial growth was quantified at 72 hpi. $n = 8$. F, CCC1 suppresses flg22-induced resistance to *Pst* DC3000. Col-0 and *ccc1-2* were pretreated with WATER or flg22 for 24 H, and then sprayed with *Pst* DC3000. Bacterial growth was determined at 72 hpi. The data in (A) to (F) represent the mean ± SE of indicated number (*n*) of biological replicates. Different letters indicate significant differences ($P < 0.05$, two-tailed *t* test) compared with wild-type plants or mock treatment. All experiments were repeated at least two times with similar results.

to the wild-type level (Fig. 1D). Altogether, the pharmacological and genetic evidence suggests that CCC1 positively regulates basal disease resistance.

ccc1 Mutants Show Reduced Levels of ETI against *Pst* DC3000 *avrRpm1*

Avirulent *Pst* DC3000 strains expressing pathogen effectors rapidly induce ETI responses in Arabidopsis plants carrying a functional copy of the corresponding

R gene, and thus are unable to multiply aggressively or cause disease in these plants (Hammond-Kosack and Jones, 1996). To test whether CCC1 is involved in R protein-induced ETI, we assessed whether resistance to avirulent *Pst* DC3000 carrying the *avrRpm1* gene was affected in *ccc1* mutants. Therefore, wild type, ccc1 mutants, and complementation lines were spray-inoculated with *Pst* DC3000 *avrRpm1* and bacterial titers were determined at 3 and 72 hpi. Although *ccc1* mutant plants were more susceptible to avirulent *Pst* DC3000 *avrRpm1* (Fig. 2A), the CL-5 and CL-7 lines
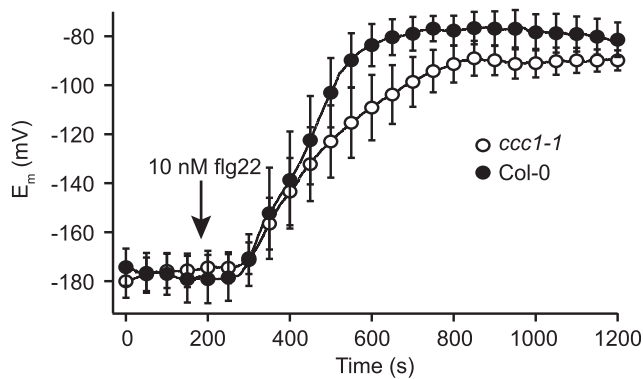
Figure 4. CCC1 is not required for PM depolarization. Flg22 (10 nM)-triggered PM depolarization in wild-type (*n* = 6) and *ccc1-1* mutant (*n* = 10) mesophyll cells are shown. The data represent the mean ± SE of indicated number (*n*) of biological replicates. These experiments were repeated at least two times with similar results.

exhibited wild-type levels of bacteria. This result indicates that CCC1 is involved in RPM1-mediated ETI.

ETI often culminates in the development of hypersensitive cell death corresponding with bacterial growth inhibition (Cui et al., 2015). To determine whether hypersensitive cell death was impaired in *ccc1* mutants, we quantified cell death in wild-type and *ccc1* mutant plants by ion leakage assays. As shown in Figure 2B, the extent of ion leakage was clearly lower in *ccc1-2* mutant leaf discs when compared with those of wild-type plants. Taken together, we conclude that *CCC1* acts as a positive regulator of ETI against *Pst* DC3000 *avrRpm1*.

CCC1 Modulates PTI Responses and Disease Resistance to *Pst* DC3000 *hrcC⁻*

Because PTI plays an important role in host defense against infections by a broad spectrum of pathogens (Wu et al., 2014; Yu et al., 2017), we tested whether CCC1 is involved in PTI responses. We first measured flg22-triggered ROS production in wild type, *ccc1* mutants, and complementation lines. As shown in Figure 3A, in contrast with wild type and complementation lines, leaf discs from *ccc1* mutant plants produced more ROS than those from wild-type plants in response to flg22 (Fig. 3A). Next, we measured the expression levels of PTI marker genes *NHL10* and *FRK1* at 1 h after flg22 or WATER (mock) treatment. As shown in Figure 3B, the induction of *NHL10* and *FRK1* was moderately enhanced in *ccc1-2* mutant compared with wild-type plants (Fig. 3B). Because SA is an important hormone in resistance against hemibiotrophic pathogens (Glazebrook, 2005), we quantified free SA accumulation in mock- or flg22-challenged Col-0 and *ccc1-2* seedlings. Relative to wild-type plants, *ccc1-2* showed an almost 2-fold increase in flg22-induced SA amounts 24 h after treatment (Fig. 3C). In summary, these results demonstrate that *CCC1* mutation

leads to enhanced flg22-induced responses, suggesting that CCC1 is a negative regulator of PTI responses.

To further investigate the role of CCC1 in PTI, 2-week-old Col-0, *ccc1-1*, *ccc1-2*, CL-5, and CL-7 seedlings were flood-inoculated with nonpathogenic *Pst* DC3000 *hrcC⁻*, which lacks the T3SS and only triggers PTI (Yuan and He, 1996). In line with higher PTI responses in *ccc1* mutant plants, less bacterial growth was observed in *ccc1* mutant plants at 72 hpi, whereas CL-5 and CL-7 showed wild-type levels of bacterial growth (Fig. 3D). We next tested whether the NKCC cotransporter activity of CCC1 is also essential for resistance to *Pst* DC3000 *hrcC⁻*. Wild-type and *ccc1-2* seedlings grown on half-strength Murashige and Skoog (MS) plates with ethanol (mock) or bumetanide were challenged with *Pst* DC3000 *hrcC⁻*, and the bacterial titer was measured at 72 hpi. As shown in Figure 3E, bacterial growth was strongly suppressed in wild-type seedlings treated with bumetanide (Fig. 3E). However, bumetanide- or ethanol (mock)-treated *ccc1-2* seedings showed similar bacterial cfu (Fig. 3E), indicating that bumetanide acts specifically on CCC1, and the NKCC cotransporter activity of CCC1 is involved in resistance to *Pst* DC3000 *hrcC⁻*. Taken together, these data demonstrate a negative regulatory role of CCC1 in PTI.

CCC1 Suppresses flg22-Induced Resistance to *Pst* DC3000

To determine whether CCC1 regulates flg22-induced resistance to *Pst* DC3000, we carried out flg22-induced protection assays. Wild-type and *ccc1-2* mutant plants were pretreated either with flg22 or WATER (mock) for 24 h before inoculation with *Pst* DC3000 (Zipfel et al., 2004). As shown in Figure 3F, bacterial growth was strongly suppressed in both wild-type and *ccc1-2* mutant plants pretreated with flg22. Although the *ccc1-2* mutant plants allowed more bacterial growth than wild-type plants in the absence of flg22 treatment, *ccc1-2* mutant plants were indistinguishable from wild type that received flg22 pretreatment. This result supports the negative regulatory role of CCC1 in flg22-induced resistance to *Pst* DC3000.

CCC1 Is Not Required for PM Depolarization

Changes in cellular ion concentration by ion fluxes across the PM are important mediators in inducing plant defense responses (Jabs et al., 1997; Jeworutzki et al., 2010). Because CCC1 is an ion transporter, the altered resistance to *Pst* DC3000 infection of *ccc1* mutant plants prompted us to investigate whether CCC1 is involved in flg22-induced PM depolarization (Jeworutzki et al., 2010). As shown in Figure 4, 10 nM flg22 triggered a strong PM depolarization after a delay of approximately 2 min in both wild-type and *ccc1* mesophyll cells. However, no major differences in the magnitude and velocity of the PM depolarization was observed between wild-type and *ccc1-1* mutant plants,
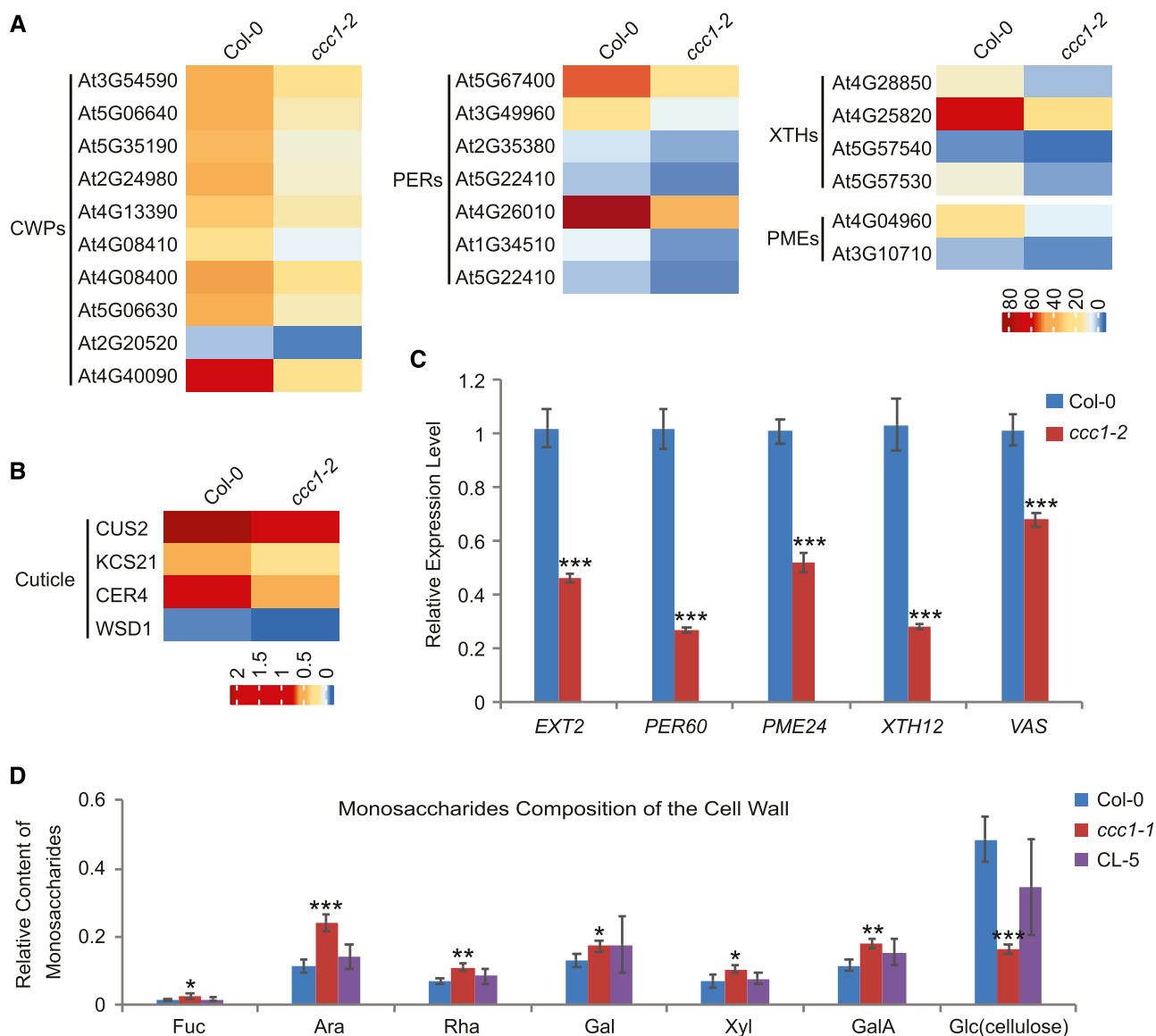
Figure 5. *ccc1* **m**utants show lower expression level of cell wall modification and cuticle biosynthesis genes and altered cell wall composition. A and B, Heat maps of cell wall-related genes (A) and cuticle biosynthesis genes (B) in Col-0 and *ccc1-2* mutant. The original TPM values were subjected to generate the heat map. Red color indicates higher, and blue color is for lower expression. CWPs, cell wall structural proteins; PERs, peroxidases; PMEs, pectin methyl esterases; XTHs, xyloglucan endo-transglucosylase/ hydrolases. C, RT-qPCR validation of CCC1-regulated cuticle and cell wall-related genes. Gene expression was normalized to *UBQ10*. D, Monosaccharides composition of the cell wall in AIR extracted from wild-type plants, *ccc1-1* mutant, and complementation line CL-5. Bars in (C) and (D) represent means ± SE of three biological replicates. Statistical differences in (C) and (D) were detected based on a two-tailed Student's *t* test. *P value < 0.05, **P value < 0.01, ***P value < 0.001 when compared with the wild type.

demonstrating that CCC1 is not required for PM depolarization.

ccc1 Mutants Show Reduced Expression Levels of Cell Wall Modification and Cuticle Biosynthesis Genes

To elucidate the mechanism underlying the role of CCC1 in plant immunity, we performed global transcriptome analysis by RNA sequencing (RNA-Seq) to identify CCC1-regulated genes in 14-d-old Col-0 and *ccc1-2* seedlings. Samples from three independent biological repeats were collected for RNA-Seq. Using a 2-fold change threshold (P value < 0.05), 220 genes were shown to be differentially expressed (29 genes upregulated and 191 down-regulated) in *ccc1-2* in comparison with wild type (Supplemental Table S1). Gene ontology enrichment analysis of the 220 genes

Table 1. *Defense-related genes were constitutively down-regulated in the* ccc1-2 *mutants*

Gene Description	Locus	Fold Change (Wild type/*ccc1-2*)	Reference
PR1	AT2G14610	3.10	Delaney et al., 1994; Glazebrook et al., 1996
PR2	AT3G57260	9.35	Kauffmann et al., 1987
PR3 (CHI-B)	AT3G12500	2.02	Legrand et al., 1987
PBS3	AT5G13320	3.46	Nobuta et al., 2007
WRKY70	AT3G56400	2.06	Jiang et al., 2016
FMO1	AT1G19250	1.93	Bernsdorff et al., 2016
ERF14	AT1G04370	5.73	Oñate-Sánchez et al., 2007
AtRLP23	AT2G32680	2.46	Albert et al., 2015
CRK32	AT4G11480	7.77	Bourdais et al., 2015
CRK23	AT4G23310	7.36	Bourdais et al., 2015
RBA1	AT1G47370	2.86	Nishimura et al., 2017
Terpene synthase	AT1G61120	4.44	Attaran et al., 2008

differentially expressed in the *ccc1-2* mutant showed striking enrichment in categories of plant cell wall functions. These genes include 10 cell wall structural proteins (5 extensins, 3 Prorich proteins, and 2 arabinogalactans), 7 peroxidases, 2 pectin methylesterases, and 4 xyloglucan endotransglucosylases/hydrolases (Fig. 5A). Moreover, we found 4 down-regulated genes to be involved in cuticle deposition (Fig. 5B), including KCS21 (Costaglioli et al., 2005), which is involved in the biosynthesis of long chain fatty acids; CUS2 (Hong et al., 2017), which is crucial for maintenance of cuticular ridges; and CER4 (Rowland et al., 2006) and WSD1 (Li et al., 2008), which are involved in cuticular wax

biosynthesis. Some genes were chosen and their expression patterns assessed by RT-qPCR analysis in wild-type and *ccc1-2* mutant plants. The results, shown in Figure 5C, support the reliability of our RNA-Seq data. Overall, these data demonstrate that loss-of-function of *CCC1* causes the repression of genes associated with the biosynthesis and modification of cell walls and cuticles.

ccc1 Mutants Exhibit Altered Cell Wall Composition

Considering the important role of the cell wall in defense responses and the over-representation of cell wall function-related genes among the down-regulated genes in the *ccc1-2* mutant (Fig. 5A; Supplemental Table S1), we decided to analyze the cell wall composition of *ccc1* mutant. As shown in Figure 5D, we determined cellulose content and the levels of noncellulosic neutral monosaccharides and GalA of extractable homogalacturonan of leaves from nontreated wild type, the *ccc1-1* mutant, and the CL-5 complementation line. The results show that the relative cellulose content was much lower in the *ccc1-1* mutant than in wild-type or complemented plants. All neutral sugars except Glc were higher in the cellulosic fraction in *ccc1-1* compared with wild-type and complemented cell walls, probably due to the significant loss of cellulose in *ccc1-1* cell walls (Fig. 5D). Taken together, these results demonstrate a function of CCC1 in regulating cell wall composition.

Defense-Related Genes and Antimicrobial Molecule Biosynthesis Genes Are Constitutively Suppressed in *ccc1-2* Mutant Plants

Our RNA-Seq data identified several constitutively down-regulated genes in *ccc1-2* mutants, which had previously been implicated in plant defense (Table 1). Among these, the three *PR* genes *PR1*, *PR2*, and *CHI-B* are rapidly induced and their products secreted to the plant apoplast as part of the host immunity to combat extracellular pathogens such as *P. syringae* (van Loon et al., 2006; Kalde et al., 2007). Besides *PR* genes, *PBS3*,

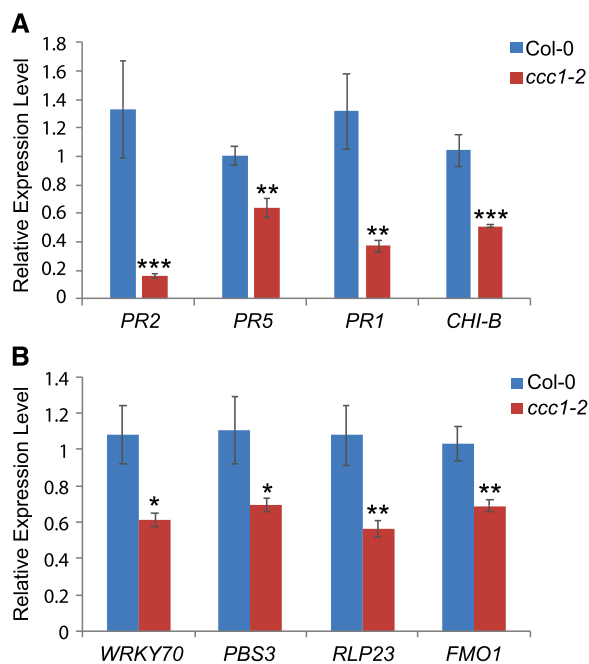**Figure 6.** Defense-related genes are constitutively suppressed in *ccc1-2* mutant. A and B, RT-qPCR validation of CCC1-regulated *PR* genes and other defense genes. Gene expression was normalized to *UBQ10*. The data are the means ± SE; *n* = 3. Statistical differences were detected based on a two-tailed Student's *t* test. *P value < 0.05, **P value < 0.01, ***P value < 0.001 when compared with the wild type.
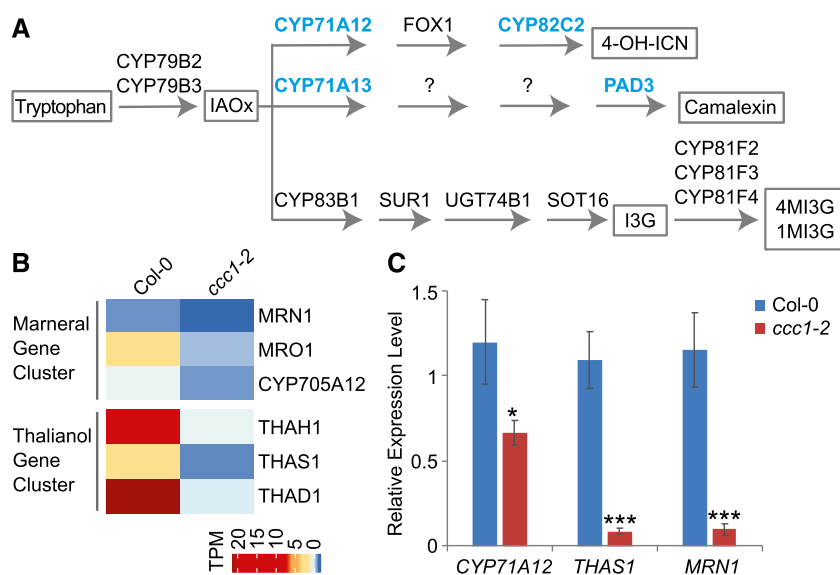
Figure 7. Antimicrobial chemical compounds biosynthesis genes are constitutively down-regulated in *ccc1-2* mutant. A, Biosynthetic pathways of Trp-derived antimicrobials camalexin, 4-OH-ICN, and indole glucosinolates in Arabidopsis (Rajniak et al., 2015; Xu et al., 2016). Key genes which are down-regulated in *ccc1-2* mutant plants are in bold and cyan color. B, Heat maps of marneral and thalianol gene cluster in Col-0 and *ccc1-2* mutant. The original TPM values were used to generate the heat map. Red color indicates higher, and blue color is for lower expression. C, RT-qPCR validation of CCC1-regulated chemical compound synthesis genes. Gene expression was normalized to *UBQ10*. The data are the means ± se; n = 3. Statistical differences were detected based on a two-tailed Student's t test. *P value < 0.05, and ***P value < 0.001 when compared with the wild type.

WRKY70, FMO1, and *RLP23* function in plant defense against *P. syringae* strains (Nobuta et al., 2007; Albert et al., 2015; Bernsdorff et al., 2016; Jiang et al., 2016). Expression levels of several defense-related and *PR* genes were validated by RT-qPCR (Fig. 6). The reduced expression of these crucial defense genes corroborates the differential susceptibility of *ccc1* mutant plants to bacterial pathogens.

The RNA-Seq data also showed repression of essential genes for the biosynthesis of antimicrobial compounds including camalexin, 4-OH-ICN, marneral, and thalianol in *ccc1* mutant plants (Fig. 7, A and B). RT-qPCR results confirmed that these genes were down-regulated in *ccc1-2* mutant plants (Fig. 7C). In addition, a large number of genes involved in the production of several main families of antimicrobial peptides (AMPs) were constitutively down-regulated in *ccc1-2* mutant compared with wild-type plants. These AMPs include 3 thionins, 7 defensins, 1 hevein, 1 knottin, and 22 lipid transfer proteins (Table 2). Taken together, mutation of *CCC1* affects a large number of biosynthetic pathways for the production of antimicrobial peptides and compounds, highlighting an important role of CCC1 as a positive regulator of defense signaling.

DISCUSSION

Ion fluxes are one of the earliest physiological responses of plant cells to PAMP recognition and play an important role in defense response induction. However, only a scant number of channels/transporters have been analyzed for their contribution to plant immunity. Using pharmacological, genetic, and biochemical analyses, we show here that the Golgi- and TGN-localized cation-chloride cotransporter CCC1 positively regulates basal resistance and ETI toward *Pst* DC3000 in Arabidopsis. However, CCC1 deficiency increases PTI responses and flg22-induced resistance to

Pst DC3000. These results demonstrate a complex dual regulatory role of intracellular ion transporters in plant immunity.

Plant cuticles and cell walls provide a physical barrier to protect plants from desiccation (Cantu et al., 2008; Serrano et al., 2014). The increased availability of water supports apoplastic pathogen growth and pathogenicity (Schreiber et al., 2005; Xin et al., 2016) and some cuticle-defective mutants of Arabidopsis increase leaf cuticle permeability and susceptibility to *P. syringae* infection (Xiao et al., 2004; Tang et al., 2007). Our comparative transcriptomic analysis of *ccc1* and wild-type plants revealed that genes involved in cuticle biosynthesis, and cell wall remodeling and modification were suppressed in *ccc1* mutant plants (Fig. 5, A–C), indicating that *CCC1* may regulate cuticle and cell wall biosynthesis and/or modification. Interestingly, rates of water the cuticle and cell walls of *ccc1* mutants were significantly higher than those of wild-type plants, as indicated by faster water loss of detached leaves and a severe water soaking phenotype under high humidity, although further experiments are necessary to determine the epidermal cell wall and/or cuticle thickness in *ccc1* mutant plants.

Quantification of the cell wall composition from wild-type plants and *ccc1* mutants showed that the composition of monosaccharides was significantly changed in *ccc1* mutants (Fig. 5D). Interestingly, CCC1 has been shown to be an endomembrane protein, which is localized to the Golgi and TGN (Henderson et al., 2015). The possibility that CCC1 regulates ion levels in the Golgi and consequently cell wall biosynthesis in the Golgi apparatus (Sandhu et al., 2009) needs to be tested in future studies.

Our RNA-Seq data showed the down-regulation of essential genes involved in the biosynthesis of the phytoalexins camalexin and 4-OH-ICN in *ccc1* mutant plants (Fig. 7A). Camalexin, one of the main phytoalexins accumulating in Arabidopsis, not only shows

Table 2. *Genes involved in antimicrobial peptides production are repressed in* ccc1-2 *mutant plants compared with wild-type plants*

Family and Gene Description	Locus	Fold Change (Wild type/ccc1-2)	Reference
Thionins			
Thi2.1	AT1G72260	3.41	Carmona et al., 1993; Molina et al., 1993a; Chan et al., 2005
Plant thionin family protein	AT1G11572	6.18	
Plant thionin family protein	AT1G66100	1.95	
Defensins			
PDF1.2a	AT5G44420	3.61	Terras et al., 1993; Segura et al., 1998; Spelbrink et al., 2004; De Coninck
PDF1.3	AT2G26010	1.93	et al., 2010; Rogozhin et al., 2011
PDF1.2b	AT2G26020	1.95	
PDF1.2c	AT5G44430	3.94	
PDF1.5	AT1G55010	3.07	
PDF1.1	AT1G75830	2.82	
PDF2.1	AT2G02120	2.29	
Hevein			
HEVEIN-LIKE	AT3G04720	1.64	Kiba et al., 2003
Knottin			
Scorpion toxin-like knottin superfamily protein	AT2G43535	1.88	Chouabe et al., 2011
Lipid transfer proteins			
LTP3	AT5G59320	1.57	Molina et al., 1993b; Segura et al., 1993; Molina and García-Olmedo, 1997;
LTP8	AT2G18370	1.75	Patkar and Chattoo, 2006; Sarowar et al., 2009; Finkina et al., 2016
Protease inhibitor/ antimicrobial peptide LTP	AT4G22666	2.06	
Protease inhibitor/ antimicrobial peptide LTP	AT4G33550	1.73	
Protease inhibitor/ antimicrobial peptide LTP	AT5G46890	3.98	
Protease inhibitor/ antimicrobial peptide LTP	AT2G37870	5.28	
Protease inhibitor/ antimicrobial peptide LTP	AT3G22570	2.23	
Protease inhibitor/ antimicrobial peptide LTP	AT3G22620	1.55	
Protease inhibitor/ antimicrobial peptide LTP	AT5G05960	1.52	
Protease inhibitor/ antimicrobial peptide LTP	AT4G15160	1.7	
Protease inhibitor/ antimicrobial peptide LTP	AT2G44300	1.51	
Protease inhibitor/ antimicrobial peptide LTP	AT3G53980	1.98	
Protease inhibitor/ antimicrobial peptide LTP	AT3G58550	1.74	
AIR1B	AT4G12545	5.24	
Protease inhibitor/ antimicrobial peptide LTP	AT4G22610	1.62	
AIR1	AT4G12550	5.58	
ROSY1	AT2G16005	2.79	
ABCA6	AT3G47770	2.76	
AZI5	AT4G12510	3.34	
Lipid transfer-like protein VAS	AT5G13900	2.54	
Protease inhibitor/ antimicrobial peptide LTP	AT4G12520	2	
Protease inhibitor/ antimicrobial peptide LTP	AT5G46900	2.75	

antifungal activity but also functions in the antibacterial defense response (Tsuji et al., 1992; Rogers et al., 1996; Zhang et al., 2014; Rajniak et al., 2015). 4-OH-ICN, which is a recently recognized cyanogenic metabolite in Arabidopsis, is required for resistance against *Pst DC3000* (Rajniak et al., 2015). T-DNA insertion mutants of four biosynthesis genes of camalexin and 4-OH-ICN, which are *CYP71A12, CYP82C2, CYP71A13,*

and *PAD3*, indicate that these compounds contribute nonredundantly to plant resistance against *Pst* DC3000 (Rajniak et al., 2015). However, production of Trp-derived glucosinolates does not seem to be affected by mutation of *CCC1* (Fig. 7A). Upon attack by pathogens, land plants also produce a heterogeneous group of phytoantipicins, which show inhibitory effects to a variety of invading microbes (González-Lamothe et al., 2009). Two gene clusters, which are required for the synthesis of the phytoanticipins marneral and thalianol, were also suppressed in *ccc1* mutants (Fig. 7B). Marneral and thalianol have been proposed to function in plant defense in Arabidopsis by analogy with well characterized phytoanticipins from cereals (Supplemental Fig. S2), although genetic evidence for their involvement in plant immunity is still lacking (Field and Osbourn, 2008; Chu et al., 2011; Field et al., 2011).

AMPs are secreted peptides that kill a variety of invading pathogens by disrupting the membranes or inactivating their ribosomes (García-Olmedo et al., 1998; Chen et al., 2002; Shai, 2002; Marmiroli and Maestri, 2014). The RNA-Seq data showed that a large number of genes involved in the production of AMPs are constitutively down-regulated in *ccc1* mutant compared with wild-type plants. Transgenic plants which constitutively express some AMPs such as thionin (Thi2.1) and lipid transfer proteins have been shown to have enhanced resistance to *P. syringae* in several plant species (Molina and García-Olmedo, 1997; Chan et al., 2005; Sarowar et al., 2009). Defensins are best known for their antifungal activities, but purified defensins from spinach also showed in vitro antibacterial activity (Segura et al., 1998).

Taken together, CCC1 affects both the biosynthesis and modification of plant cell walls and cuticles as well as many antimicrobial compounds, all of which might explain the compromised pathogen resistance phenotype of *ccc1* mutants. A current denominator for these diverse compounds is their necessary transit through the Golgi and TGN to be secreted into the extracellular space. Most immune signaling processes related to ion fluxes have focused on the PM, where PAMP- pattern recognition receptor interaction takes place to trigger intracellular defense signaling pathways (Roelfsema et al., 2012). At present, it is not clear whether ion fluxes across the Golgi and TGN membranes are regulated in response to pathogen signals. However, the Golgi-TGN network clearly serves as a hub for protein trafficking and secretion of a number of substances, including cell wall and antimicrobial components (LaMontagne and Heese, 2017; Uemura et al., 2019), and further studies are necessary to clarify whether CCC1 is involved in the sorting of immune-related products in the Golgi-TGN network.

CONCLUSION

Plant cuticles, cell walls, and secreted antimicrobial compounds constitute the first line of plant defense against harmful pathogens. We reported here that *CCC1* mutation caused the suppression of cuticle and cell wall–related genes and genes for the biosynthesis of antimicrobial peptides and defense chemicals. Chemical analyses of cell walls from wild-type and *ccc1* mutant plants showed that cell wall composition was strongly changed in *ccc1* mutants compared with that in wild-type plants. Consistently, *ccc1* mutant plants were more susceptible to the virulent bacterial pathogen *P. syringae* (*Pst*) DC3000. In addition, using a pharmacological approach, the NKCC cotransporter activity of CCC1 was demonstrated to be essential for the functionality of CCC1 in the regulation of PTI and resistance to *Pst* DC3000. These results revealed the function of the Golgi-localized ion transporter CCC1 in the reinforcement of plant structural and chemical barriers in plant immunity.

MATERIALS AND METHODS

Plant Materials and Growth Conditions

Arabidopsis (*Arabidopsis thaliana*) ecotype Col-0 was used as wild type in this study. *ccc1-1* (SALK_048175) and *ccc1-2* (SALK_145300) T-DNA insertion lines were obtained from Nottingham Arabidopsis Stock Centre. Homozygous T-DNA insertion lines were screened by PCR-based genotyping using primers listed in Supplemental Table S2. Transgenic plants expressing pUBQ10:CCC1-GFP in the background of *ccc1-2* mutant were generated in this study. Arabidopsis plants were grown individually in Jiffy-7 pellet (Jiffy Products International) in a controlled cultivation chamber with a 12-h-d (110 μmol m^{-2} s^{-1}) / 12-h-night cycle and a relative humidity of 60%. Day and night temperatures were set to 22°C and 20°C, respectively. Four-week-old plants were used for bacterial disease and ROS burst assays. For microelectrode studies, plants were grown for 5 to 6 weeks in a growth chamber, with 60% relative humidity, a day/night cycle of 12/12 h, temperatures of 21°C/18°C, and a photon flux density of 100 μmol m^{-2} s^{-1}. For MAPK, RT-qPCR assay, RNA-Seq, SA quantification, surface-sterilized seeds were vernalized at 4°C in the dark for 3 d and then germinated on half-strength MS (Sigma M6899) plates, containing 0.5% (w/v) Suc (Sigma S5016), 1% (w/v) agar (Sigma A1296), and 0.05% (w/v) MES (Sigma M8250), grown at 23°C, 60% humidity, and 125 μmol m^{-2} s^{-1} light with a 16-h-light / 8-h-dark photoperiod. The plants were transferred to a new 60 mm × 60 mm petri dish with 10 mL half-strength MS medium overnight before treatment. Then the plants were treated with flg22 for the indicated amounts of time. For MAPK assays, 10-d-old seedlings were used. For RT-qPCR assay, RNA-Seq, SA quantification, 14-d-old seedlings were used.

Plasmid Construction

CCC1 CDS was amplified from Col-0 cDNA using Phusion High-Fidelity DNA Polymerase (NEB), the entry clone *CCC1*-pDONR207 was generated using Gateway BP Clonase II Enzyme mix (Invitrogen). pUBC-GFP-DEST (Grefen et al., 2010) was used to generate complementation construct pUBQ10:CCC1-GFP using Gateway LR Clonase II Enzyme Mix (Invitrogen). All the constructs were verified by Sanger sequencing and primers are listed in Supplemental Table S2.

Bacterial Disease Assays

Spray-inoculation, syringe-infiltrated inoculation and flooding-inoculation were used in this study (Jiang et al., 2019). Briefly, different *Pst* DC3000 strains were cultivated at 28°C for 24 h on King Agar B (Sigma 60786) plates containing appropriate antibiotics. Bacteria were suspended and adjusted to different final densities with 10 mM MgSO$_4$. For spray-inoculation, 4-week-old plants were sprayed with bacterial suspensions of optical density at wavelength of 600 nm (OD$_{600}$) = 0.2 (~1×10^8 cfu/mL), with 0.04% (w/v) Silwet L-77 (LEHLE SEEDS) added, and then covered with a clear plastic dome immediately for disease to develop. For syringe-infiltration, bacteria were further diluted to cell densities

of 1×10^5 cfu/mL (OD_{600} = 0.0002). Leaves of 4-week-old plants were hand-infiltrated with the bacterial suspension using a needleless syringe. Infiltrated plants were first kept under low humidity for 2 h to help water to evaporate, and then covered with the plastic dome. For flg22 protection assay, 4-week-old plants were spray-inoculated with 2 mm flg22, or WATER as a control, 24 h before being sprayed with *Pst* DC3000 (1×10^8 cfu/mL, OD = 0.2). In planta bacterial growth was determined at 3 and 72 hpi. Three leaves were detached from each plant, sterilized in 75% (v/v) ethanol for 10 s, and rinsed in sterile distilled water twice. One leaf disc was taken using a cork borer (0.25 inch in diameter) from each leaf and pooled together, and ground in 10 mm $MgSO_4$ using a TissueLyser (Qiagen) with three grinding beads in each tube at a frequency of 27 times/s for 3 min. Serial dilutions were plated on lysogeny broth agar plates with appropriate antibiotics, which were kept at 28°C for 24 h before colonies were counted. For flood inoculation, 14-d-old seedlings on half-strength MS agar plates were flood-inoculated according to the protocol published by Ishiga and colleagues with 1×10^7 cfu/mL of *Pst* DC3000 *hrcC*⁻ (Ishiga et al., 2011).

Ion Leakage Assay

Ion leakage from leaf discs of wild type and *ccc1-2* mutants was monitored as described previously (Hatsugai et al., 2016). *Pst* DC3000 *avrRpm1* were cultivated at 28°C for 24 h on King Agar B (Sigma 60786) plates containing 50 mg/L rifampicin and 30 mg/L kanamycin before plant infection. Bacteria was resuspended at 5×10^7 cfu/mL in WATER and infiltrated into leaves of 4-week-old wild-type and *ccc1-2* plants. Fifteen leaf discs were collected from leaves immediately after bacterial infiltration and washed in 10 mL of WATER for 30 min. Then the leaf discs were transferred into 10 mL fresh WATER and incubated in a shaker at 22°C. The conductivity of WATER was measured at the indicated time points using an VWR conductivity meter (PC 5000L).

ROS Burst Assay

ROS burst was measured using a luminol-based assay. Leaf discs (0.25 inch in diameter) were incubated overnight in a white 96-well plate (Costar, Fisher Scientific) containing sterile WATER to reduce wounding response. The next day, WATER was carefully removed and leaf discs were floated on 100 μL of Elicitation Solution (34 ug/mL luminol, 20 μg/mL horseradish peroxidase, and 1 μM flg22). Luminescence was detected with a TECAN Infinite 200 PRO microplate reader using integration intervals of 1 to 1.5 s. Each treatment had a minimum of eight samples. For bumetanide treatment, wild-type leaf discs were floated on 100 μL of the Elicitation Solution with application of ethanol or 100 nM bumetanide. The leaf discs were vacuumed for 5 min and luminescence was detected with a TECAN Infinite 200 PRO microplate reader as mentioned above.

Quantification of SA

SA quantification was done according to a method described previously (Forcat et al., 2008). Fourteen-day-old Arabidopsis Col-0 and *ccc1-2* seedlings were lyophilized and ground into powder. About 5 mg dry weight of powdered tissues were extracted with 400 μL of 10% (v/v) methanol containing 1% (v/v) acetic acid twice. $^2H_4$-SA (11.1 ng; OlchemIm, Olomouc) was added as an internal standard. The supernatants were filtered through 0.22 μm polytetrafluoroethylene filters before analyzing on liquid chromatography with tandem mass spectrometry. Analysis of SA was performed by using an Agilent 1200 HPLC (Agilent Technologies) coupled to a Q-TRAP 5500 MS (AB SCIEX) with an electrospray source. Chromatographic separation was carried out on a Phenomenex (Torrance) Gemini C18 (150 × 2.0 mm, 5 μm) column with mobile phases of water/acetonitrile (95/5, v/v; A) and acetonitrile/water (5/95, v/v; B) at 35°C. The gradient used was 0 to 20 min, 0% to 100% B; 20 to 25 min, 100%B; 25 to 26 min, 100% to 0% B; 26 to 36 min, 0% B. MS was operated in negative ionization mode. The mass spectrometry conditions were as follows: temperature, 500°C; ion source gas 1, 50 psi; ion source gas 2, 60 psi; ion spray voltage, −4500 V; curtain gas, 40 psi; collision gas, medium; DP, −25 V; EP, −9; CXP, −2; and CE, −38. Multiple Reaction Monitoring of ion pairs for labeled and endogenous SA using following mass transitions: [$^2H_4$]SA 141 > 97, SA 137 > 93. Data were acquired and analyzed using Analyst 1.4 software (Applied Biosystems).

PM Potential Measurements

The central vein of Arabidopsis leaves was removed with a razor blade and the adaxial epidermis was peeled, whereas the remainder of the leaf was cut into a 1 cm² square that was attached to the bottom of a petri dish with double sided adhesive tape. The petri dish was filled with a solution containing 0.1 mm KCl, 1 mm $CaCl_2$, and 1 mm MES/BTP pH 6.0. Mesophyll cells were impaled with single barreled microelectrodes, pulled from glass capillaries (o.d. 1 mm, i.d. 0.58 mm, Hilgenberg; https://www.hilgenberg-gmbh.de), using a laser puller (P2000, Sutter Intruments, https://www.sutter.com). The electrodes were filled with 300 mm KCl and had a tip resistance of approximately 60 MΩ and a capillary filled with 300 mm KCl and plugged with 2% (w/v) agarose in 300 mm KCl, which served as a reference electrode. The electrode and reference were coupled to Ag/AgCl half cells and a Bio-Logic micro electrode amplifier (CA 100, https://www.bio-logic.net/), equipped with a HS-180 headstage. The microelectrode was impaled into mesophyll cells with use of a MM3A micromanipulator (Kleindiek, https://www.kleindiek.com). The voltage data were filtered with a Bessel filter (LPF 202A; Warner Instruments Corp., www.warneronline.com) and sampled at 0.1 Hz with WinEDR software (Dempster, 1997; University of Strathclyde, https://www.strath.ac.uk), using an ITC-18 Interface (Instrutech Corp.).

RNA Extraction and RT-qPCR Analysis

Two-week-old seedlings were treated with 1 μM flg22 for 1 h. Total RNA was isolated from the seedling samples using NucleoSpin RNA Plant kit (Macherey Nagel) following the manufacturer's instructions. Total RNA (2 μg) were then used for first-strand cDNA synthesis using SuperScript III First-Strand Synthesis SuperMix (Invitrogen) with oligo(dT) primer. RT-qPCR was performed with Power SYBR Green PCR Master Mix (Applied Biosystems) on a StepOnePlus Real-Time PCR System (Applied Biosystems) following standard protocol. The expression levels of interest genes were normalized to At4g05320 (*UBQ10*). Primers for RT-qPCR were listed in Supplemental Table S2.

RNA-Seq and Transcriptome Analysis

Two-week-old Col-0 and *ccc1-2* seedlings were collected for RNA-Seq. Total RNA (100 ng) were used for RNA-Seq library preparation, which was performed in KAUST Bioscience Core Lab using TruSeq Stranded mRNA LT Sample Prep Kit following manufacturer's instructions (Illumina). Sequencing was performed on an Illumina Hi-Seq 4000 platform with 150-nucleotide paired-end reads. Before the analysis of RNA-Seq data, the sequenced reads were quality-checked using FastQC v0.11.3 (Andrews, 2018). Because of the good quality of the sequencing data, we skipped the trimming process to avoid any potential biases (Williams et al., 2016). To quantify the expression level of genes, a total of 392 million reads were pseudo-aligned to the publicly available TAIR10 Arabidopsis transcriptome (release 34) using kallisto v0.43.0 (Bray et al., 2016). The estimated read counts and calculated transcripts per million (TPM) were subsequently passed to sleuth v0.28.1 (Pimentel et al., 2017) for differential expression analysis. Significantly differentially expressed genes were identified based on a cutoff of fold-change > 2 and q-value < 0.05. Gene ontology enrichment analysis was conducted using clusterProfiler (Yu et al., 2012) and Pathview (Luo and Brouwer, 2013).

Cell Wall Analysis

Analyses were performed on 4-d-old dark-grown hypocotyls using an alcohol-insoluble residue (AIR) prepared as follows. Freshly collected samples were submerged into 96% (v/v) ethanol, grinded, and incubated for 30 min at 70°C. The pellet was then washed twice with 96% (v/v) ethanol and once with acetone. The remaining pellet of AIR was dried in a fume hood overnight at room temperature. The monosaccharide composition of the noncellulosic fraction was determined by hydrolysis of AIR with 2 m TFA for 1 h at 120°C. After cooling and centrifugation, the supernatant was dried under a vacuum, resuspended in 200 μL of water, and retained for analysis. To obtain the Glc content of the crystalline cellulose fraction, the TFA-insoluble pellet was further hydrolyzed with 72% (v/v) sulfuric acid for 1 h at room temperature. The sulfuric acid was then diluted to 1 m with water and the samples incubated at 100°C for 3 h. All samples were filtered using a 20-μm filter caps, and quantified by HPAEC-PAD on a Dionex ICS-5000 instrument (ThermoFisher Scientific) as described (Fang et al., 2016).

Accession Numbers

Sequencing data of RNA-seq were deposited in the National Center for Biotechnology Information Sequence Read Archive under BioProject code PRJNA589953.

Supplemental Data

The following supplemental materials are available.

Supplemental Figure S1. Characterization of CCC1 T-DNA knockout lines and complementation transgenic lines.

Supplemental Figure S2. Triterpene biosynthetic pathways in Arabidopsis and Oat.

Supplemental Table S1. Differential expressed genes in wild type and *ccc1-2*.

Supplemental Table S2. Primers used in this study.

LITERATURE CITED

Ahuja I, Kissen R, Bones AM (2012) Phytoalexins in defense against pathogens. Trends Plant Sci 17: 73–90

Albert I, Böhm H, Albert M, Feiler CE, Imkampe J, Wallmeroth N, Brancato C, Raaymakers TM, Oome S, Zhang H, et al (2015) An RLP23-SOBIR1-BAK1 complex mediates NLP-triggered immunity. Nat Plants 1: 15140

Ali R, Ma W, Lemtiri-Chlieh F, Tsaltas D, Leng Q, von Bodman S, Berkowitz GA (2007) Death don't have no mercy and neither does calcium: Arabidopsis CYCLIC NUCLEOTIDE GATED CHANNEL2 and innate immunity. Plant Cell 19: 1081–1095

Andrews S (2018) FastQC: A quality control tool for high throughput sequence data. Babraham Bioinforma, http://www.bioinformatics.babraham.ac.uk/projects/ (April 13, 2018)

Attaran E, Rostás M, Zeier J (2008) Pseudomonas syringae elicits emission of the terpenoid (E,E)-4,8,12-trimethyl-1,3,7,11-tridecatetraene in Arabidopsis leaves via jasmonate signaling and expression of the terpene synthase TPS4. Mol Plant Microbe Interact 21: 1482–1497

Bacete L, Mélida H, Miedes E, Molina A (2017) Plant cell wall-mediated immunity: Cell wall changes trigger disease resistance responses. Plant J 12: 3218–3221

Bernsdorff F, Döring AC, Gruner K, Schuck S, Bräutigam A, Zeier J (2016) Pipecolic acid orchestrates plant systemic acquired resistance and defense priming via salicylic acid-dependent and -independent pathways. Plant Cell 28: 102–129

Bigeard J, Colcombet J, Hirt H (2015) Signaling mechanisms in pattern-triggered immunity (PTI). Mol Plant 8: 521–539

Block A, Alfano JR (2011) Plant targets for Pseudomonas syringae type III effectors: Virulence targets or guarded decoys? Curr Opin Microbiol 14: 39–46

Boudsocq M, Willmann MR, McCormack M, Lee H, Shan L, He P, Bush J, Cheng S-H, Sheen J (2010) Differential innate immune signalling via Ca²⁺ sensor protein kinases. Nature 464: 418–422

Bourdais G, Burdiak P, Gauthier A, Nitsch L, Salojärvi J, Rayapuram C, Idänheimo N, Hunter K, Kimura S, Merilo E, et al (2015) Large-scale phenomics identifies primary and fine-tuning roles for CRKs in responses related to oxidative stress. PLoS Genet 11: e1005373

Bray NL, Pimentel H, Melsted P, Pachter L (2016) Near-optimal probabilistic RNA-seq quantification. Nat Biotechnol 34: 525–527

Cantu D, Vicente AR, Labavitch JM, Bennett AB, Powell ALT (2008) Strangers in the matrix: Plant cell walls and pathogen susceptibility. Trends Plant Sci 13: 610–617

Carmona MJ, Molina A, Fernández JA, López-Fando JJ, García-Olmedo F (1993) Expression of the α-thionin gene from barley in tobacco confers enhanced resistance to bacterial pathogens. Plant J 3: 457–462

Chan Y-L, Prasad V, Sanjaya, Chen KH, Liu PC, Chan MT, Cheng CP (2005) Transgenic tomato plants expressing an Arabidopsis thionin (Thi2.1) driven by fruit-inactive promoter battle against phytophagic attack. Planta 221: 386–393

Chen K-C, Lin C-Y, Kuan C-C, Sung H-Y, Chen C-S (2002) A novel defensin encoded by a mungbean cDNA exhibits insecticidal activity against bruchid. J Agric Food Chem 50: 7258–7263

Chouabe C, Eyraud V, Da Silva P, Rahioui I, Royer C, Soulage C, Bonvallet R, Huss M, Gressent F (2011) New mode of action for a knottin protein bioinsecticide: Pea albumin 1 subunit b (PA1b) is the first peptidic inhibitor of V-ATPase. J Biol Chem 286: 36291–36296

Chu HY, Wegel E, Osbourn A (2011) From hormones to secondary metabolism: The emergence of metabolic gene clusters in plants. Plant J 66: 66–79

Clough SJ, Fengler KA, Yu IC, Lippok B, Smith RK Jr., Bent AF (2000) The Arabidopsis dnd1 "defense, no death" gene encodes a mutated cyclic nucleotide-gated ion channel. Proc Natl Acad Sci USA 97: 9323–9328

Colcombet J, Mathieu Y, Peyronnet R, Agier N, Lelièvre F, Barbier-Brygoo H, Frachisse J (2009) R-type anion channel activation is an essential step for ROS-dependent innate immune response in Arabidopsis suspension cells. Funct Plant Biol 36: 832–843

Colmenero-Flores JM, Martínez G, Gamba G, Vázquez N, Iglesias DJ, Brumós J, Talón M (2007) Identification and functional characterization of cation-chloride cotransporters in plants. Plant J 50: 278–292

Costagliolì P, Joubès J, Garcia C, Stef M, Arveiler B, Lessire R, Garbay B (2005) Profiling candidate genes involved in wax biosynthesis in Arabidopsis thaliana by microarray analysis. Biochim Biophys Acta 1734: 247–258

Cui H, Tsuda K, Parker JE (2015) Effector-triggered immunity: From pathogen perception to robust defense. Annu Rev Plant Biol 66: 487–511

Cunnac S, Chakravarthy S, Kvitko BH, Russell AB, Martin GB, Collmer A (2011) Genetic disassembly and combinatorial reassembly identify a minimal functional repertoire of type III effectors in Pseudomonas syringae. Proc Natl Acad Sci USA 108: 2975–2980

De Coninck BMA, Sels J, Venmans E, Thys W, Goderis IJWM, Carron D, Delauré SL, Cammue BPA, De Bolle MFC, Mathys J (2010) Arabidopsis thaliana plant defensin AtPDF1.1 is involved in the plant response to biotic stress. New Phytol 187: 1075–1088

Delaney TP, Uknes S, Vernooij B, Friedrich L, Weymann K, Negrotto D, Gaffney T, Gut-Rella M, Kessmann H, Ward E, Ryals J (1994) A central role of salicylic acid in plant disease resistance. Science 266: 1247–1250

Dempster J (1997) A new version of the strathclyde electrophysiology software package running within the Microsoft Windows environment. J Physiol 504: P57

Dodds PN, Rathjen JP (2010) Plant immunity: Towards an integrated view of plant-pathogen interactions. Nat Rev Genet 11: 539–548

Dou D, Zhou J-M (2012) Phytopathogen effectors subverting host immunity: Different foes, similar battleground. Cell Host Microbe 12: 484–495

Fang L, Ishikawa T, Rennie EA, Murawska GM, Lao J, Yan J, Tsai AY-L, Baidoo EEK, Xu J, Keasling JD, et al (2016) Loss of inositol phosphorylceramide sphingolipid mannosylation induces plant immune responses and reduces cellulose content in Arabidopsis. Plant Cell 28: 2991–3004

Feng F, Zhou J-M (2012) Plant-bacterial pathogen interactions mediated by type III effectors. Curr Opin Plant Biol 15: 469–476

Field B, Fiston-Lavier A-S, Kemen A, Geisler K, Quesneville H, Osbourn AE (2011) Formation of plant metabolic gene clusters within dynamic chromosomal regions. Proc Natl Acad Sci USA 108: 16116–16121

Field B, Osbourn AE (2008) Metabolic diversification--independent assembly of operon-like gene clusters in different plants. Science 320: 543–547

Finkina EI, Melnikova DN, Bogdanov IV, Ovchinnikova TV (2016) Lipid transfer proteins as components of the plant innate immune system: Structure, functions, and applications. Acta Naturae 8: 47–61

Forcat S, Bennett MH, Mansfield JW, Grant MR (2008) A rapid and robust method for simultaneously measuring changes in the phytohormones ABA, JA and SA in plants following biotic and abiotic stress. Plant Methods 4: 16

García-Olmedo F, Molina A, Alamillo JM, Rodríguez-Palenzuéla P (1998) Plant defense peptides. Biopolymers 47: 479–491

Glazebrook J (2005) Contrasting mechanisms of defense against biotrophic and necrotrophic pathogens. Annu Rev Phytopathol 43: 205–227

Glazebrook J, Rogers EE, Ausubel FM (1996) Isolation of Arabidopsis mutants with enhanced disease susceptibility by direct screening. Genetics 143: 973–982

González-Lamothe R, Mitchell G, Gattuso M, Diarra MS, Malouin F, Bouarab K (2009) Plant antimicrobial agents and their effects on plant and human pathogens. Int J Mol Sci 10: 3400–3419

Grefen C, Donald N, Hashimoto K, Kudla J, Schumacher K, Blatt MR (2010) A ubiquitin-10 promoter-based vector set for fluorescent protein tagging facilitates temporal stability and native protein distribution in transient and stable expression studies. Plant J 64: 355–365

Guo W, Zuo Z, Cheng X, Sun J, Li H, Li L, Qiu J-L (2014) The chloride channel family gene CLCd negatively regulates pathogen-associated molecular pattern (PAMP)-triggered immunity in Arabidopsis. J Exp Bot 65: 1205–1215

Guzel Deger A, Scherzer S, Nuhkat M, Kedzierska J, Kollist H, Brosché M, Unyayar S, Boudsocq M, Hedrich R, Roelfsema MRG (2015) Guard cell SLAC1-type anion channels mediate flagellin-induced stomatal closure. New Phytol 208: 162–173

Hammond-Kosack KE, Jones JD (1996) Resistance gene-dependent plant defense responses. Plant Cell 8: 1773–1791

Hatsugai N, Hillmer R, Yamaoka S, Hara-Nishimura I, Katagiri F (2016) The μ subunit of Arabidopsis adaptor protein-2 is involved in effector-triggered immunity mediated by membrane-localized resistance proteins. Mol Plant Microbe Interact 29: 345–351

Hématy K, Cherk C, Somerville S (2009) Host-pathogen warfare at the plant cell wall. Curr Opin Plant Biol 12: 406–413

Henderson SW, Wege S, Qiu J, Blackmore DH, Walker AR, Tyerman SD, Walker RR, Gilliham M (2015) Grapevine and Arabidopsis cation-chloride cotransporters localize to the golgi and trans-golgi network and indirectly influence long-distance ion transport and plant salt tolerance. Plant Physiol 169: 2215–2229

Hentschel U (2013) Plant-microbe interactions. Bot Homepage 49: 122405

Hong L, Brown J, Segerson NA, Rose JKC, Roeder AHK (2017) CUTIN SYNTHASE 2 maintains progressively developing cuticular ridges in Arabidopsis sepals. Mol Plant 10: 560–574

Hübner CA, Rust MB (2006) Physiology of cation-chloride cotransporters. Adv Mol Cell Biol 38: 241–277

Ishiga Y, Ishiga T, Uppalapati SR, Mysore KS (2011) Arabidopsis seedling flood-inoculation technique: A rapid and reliable assay for studying plant-bacterial interactions. Plant Methods 7: 32

Jabs T, Tschope M, Colling C, Hahlbrock K, Scheel D (1997) Elicitor-stimulated ion fluxes and O_2- from the oxidative burst are essential components in triggering defense gene activation and phytoalexin synthesis in parsley. Proc Natl Acad Sci USA 94: 4800–4805

Jeworutzki E, Roelfsema MRG, Anschütz U, Krol E, Elzenga JTM, Felix G, Boller T, Hedrich R, Becker D (2010) Early signaling through the Arabidopsis pattern recognition receptors FLS2 and EFR involves Ca-associated opening of plasma membrane anion channels. Plant J 62: 367–378

Jiang CH, Huang ZY, Xie P, Gu C, Li K, Wang DC, Yu YY, Fan Z-H, Wang C-J, Wang Y-P, et al (2016) Transcription factors WRKY70 and WRKY11 served as regulators in rhizobacterium Bacillus cereus AR156-induced systemic resistance to Pseudomonas syringae pv. tomato DC3000 in Arabidopsis. J Exp Bot 67: 157–174

Jiang Y, Han B, Zhang H, Mariappan KG, Bigeard J, Colcombet J, Hirt H (2019) MAP4K4 associates with BIK1 to regulate plant innate immunity. EMBO Rep 20: e47965

Jin Q, He SY (2001) Role of the Hrp pilus in type III protein secretion in Pseudomonas syringae. Science 294: 2556–2558

Johansson ON, Nilsson AK, Gustavsson MB, Backhaus T, Andersson MX, Ellerström M (2015) A quick and robust method for quantification of the hypersensitive response in plants. PeerJ 3: e1469

Jones JDG, Dangl JL (2006) The plant immune system. Nature 444: 323–329

Jurkowski GI, Smith RK Jr., Yu IC, Ham JH, Sharma SB, Klessig DF, Fengler KA, Bent AF (2004) Arabidopsis DND2, a second cyclic nucleotide-gated ion channel gene for which mutation causes the "defense, no death" phenotype. Mol Plant Microbe Interact 17: 511–520

Kalde M, Nühse TS, Findlay K, Peck SC (2007) The syntaxin SYP132 contributes to plant resistance against bacteria and secretion of pathogenesis-related protein 1. Proc Natl Acad Sci USA 104: 11850–11855

Kauffmann S, Legrand M, Geoffroy P, Fritig B (1987) Biological function of pathogenesis-related' proteins: four PR proteins of tobacco have 1,3-β-glucanase activity. EMBO J 6: 3209–3212

Kiba A, Saitoh H, Nishihara M, Omiya K, Yamamura S (2003) C-terminal domain of a hevein-like protein from Wasabia japonica has potent antimicrobial activity. Plant Cell Physiol 44: 296–303

Koers S, Guzel-Deger A, Marten I, Roelfsema MRG (2011) Barley mildew and its elicitor chitosan promote closed stomata by stimulating guard-cell S-type anion channels. Plant J 68: 670–680

Lacombe S, Rougon-Cardoso A, Sherwood E, Peeters N, Dahlbeck D, van Esse HP, Smoker M, Rallapalli G, Thomma BPHJ, Staskawicz B, et al (2010) Interfamily transfer of a plant pattern-recognition receptor confers broad-spectrum bacterial resistance. Nat Biotechnol 28: 365–369

Lamb CJ, Lawton MA, Dron M, Dixon RA (1989) Signals and transduction mechanisms for activation of plant defenses against microbial attack. Cell 56: 215–224

LaMontagne ED, Heese A (2017) Trans-Golgi network/early endosome: A central sorting station for cargo proteins in plant immunity. Curr Opin Plant Biol 40: 114–121

Legrand M, Kauffmann S, Geoffroy P, Fritig B (1987) Biological function of pathogenesis-related proteins: Four tobacco pathogenesis-related proteins are chitinases. Proc Natl Acad Sci USA 84: 6750–6754

Li F, Wu X, Lam P, Bird D, Zheng H, Samuels L, Jetter R, Kunst L (2008) Identification of the wax ester synthase/acyl-coenzyme A: Diacylglycerol acyltransferase WSD1 required for stem wax ester biosynthesis in Arabidopsis. Plant Physiol 148: 97–107

Luo W, Brouwer C (2013) Pathview: An R/Bioconductor package for pathway-based data integration and visualization. Bioinformatics 29: 1830–1831

Macho AP, Zipfel C (2015) Targeting of plant pattern recognition receptor-triggered immunity by bacterial type-III secretion system effectors. Curr Opin Microbiol 23: 14–22

Marmiroli N, Maestri E (2014) Plant peptides in defense and signaling. Peptides 56: 30–44

Molina A, García-Olmedo F (1997) Enhanced tolerance to bacterial pathogens caused by the transgenic expression of barley lipid transfer protein LTP2. Plant J 12: 669–675

Molina A, Goy PA, Fraile A, Sánchez-Monge R, García-Olmedo F (1993a) Inhibition of bacterial and fungal plant pathogens by thionins of types I and II. Plant Sci 92: 169–177

Molina A, Segura A, García-Olmedo F (1993b) Lipid transfer proteins (nsLTPs) from barley and maize leaves are potent inhibitors of bacterial and fungal plant pathogens. FEBS Lett 316: 119–122

Montillet J-L, Leonhardt N, Mondy S, Tranchimand S, Rumeau D, Boudsocq M, Garcia AV, Douki T, Bigeard J, Laurière C, et al (2013) An abscisic acid-independent oxylipin pathway controls stomatal closure and immune defense in Arabidopsis. PLoS Biol 11: e1001513

Nishimura MT, Anderson RG, Cherkis KA, Law TF, Liu QL, Machius M, Nimchuk ZL, Yang L, Chung E-H, El Kasmi F, et al (2017) TIR-only protein RBA1 recognizes a pathogen effector to regulate cell death in Arabidopsis. Proc Natl Acad Sci USA 114: E2053–E2062

Nobuta K, Okrent RA, Stoutemyer M, Rodibaugh N, Kempema L, Wildermuth MC, Innes RW (2007) The GH3 acyl adenylase family member PBS3 regulates salicylic acid-dependent defense responses in Arabidopsis. Plant Physiol 144: 1144–1156

Oñate-Sánchez L, Anderson JP, Young J, Singh KB (2007) AtERF14, a member of the ERF family of transcription factors, plays a nonredundant role in plant defense. Plant Physiol 143: 400–409

Patkar RN, Chattoo BB (2006) Transgenic indica rice expressing ns-LTP-like protein shows enhanced resistance to both fungal and bacterial pathogens. Mol Breed 17: 159–171

Pimentel H, Bray NL, Puente S, Melsted P, Pachter L (2017) Differential analysis of RNA-seq incorporating quantification uncertainty. Nat Methods 14: 687–690

Qi Z, Verma R, Gehring C, Yamaguchi Y, Zhao Y, Ryan CA, Berkowitz GA (2010) Ca^{2+} signaling by plant Arabidopsis thaliana Pep peptides depends on AtPepR1, a receptor with guanylyl cyclase activity, and cGMP-activated Ca^{2+} channels. Proc Natl Acad Sci USA 107: 21193–21198

Rajniak J, Barco B, Clay NK, Sattely ES (2015) A new cyanogenic metabolite in Arabidopsis required for inducible pathogen defence. Nature 525: 376–379

Roelfsema MRG, Hedrich R, Geiger D (2012) Anion channels: Master switches of stress responses. Trends Plant Sci 17: 221–229

Rogers EE, Glazebrook J, Ausubel FM (1996) Mode of action of the *Arabidopsis thaliana* phytoalexin camalexin and its role in *Arabidopsis-pathogen* interactions. Mol Plant Microbe Interact 9: 748–757

Rogozhin EA, Oshchepkova YI, Odintsova TI, Khadeeva NV, Veshkurova ON, Egorov TA, Grishin EV, Salikhov SI (2011) Novel antifungal defensins from *Nigella sativa* L. seeds. Plant Physiol Biochem 49: 131–137

Rowland O, Zheng H, Hepworth SR, Lam P, Jetter R, Kunst L (2006) CER4 encodes an alcohol-forming fatty acyl-coenzyme A reductase involved in cuticular wax production in Arabidopsis. Plant Physiol 142: 866–877

Sandhu APS, Randhawa GS, Dhugga KS (2009) Plant cell wall matrix polysaccharide biosynthesis. Mol Plant 2: 840–850

Sarowar S, Kim YJ, Kim KD, Hwang BK, Ok SH, Shin JS (2009) Over-expression of lipid transfer protein (LTP) genes enhances resistance to plant pathogens and LTP functions in long-distance systemic signaling in tobacco. Plant Cell Rep 28: 419–427

Schreiber L, Krimm U, Knoll D, Sayed M, Auling G, Kroppenstedt RM (2005) Plant-microbe interactions: identification of epiphytic bacteria and their ability to alter leaf surface permeability. New Phytol 166: 589–594

Schwessinger B, Zipfel C (2008) News from the frontline: Recent insights into PAMP-triggered immunity in plants. Curr Opin Plant Biol 11: 389–395

Segura A, Moreno M, García-Olmedo F (1993) Purification and anti-pathogenic activity of lipid transfer proteins (LTPs) from the leaves of Arabidopsis and spinach. FEBS Lett 332: 243–246

Segura A, Moreno M, Molina A, García-Olmedo F (1998) Novel defensin subfamily from spinach (*Spinacia oleracea*). FEBS Lett 435: 159–162

Serrano M, Coluccia F, Torres M, L'Haridon F, Métraux J-P (2014) The cuticle and plant defense to pathogens. Front Plant Sci 5: 274

Shai Y (2002) Mode of action of membrane active antimicrobial peptides. Biopolymers 66: 236–248

Spelbrink RG, Dilmac N, Allen A, Smith TJ, Shah DM, Hockerman GH (2004) Differential antifungal and calcium channel-blocking activity among structurally related plant defensins. Plant Physiol 135: 2055–2067

Tang D, Simonich MT, Innes RW (2007) Mutations in LACS2, a long-chain acyl-coenzyme A synthetase, enhance susceptibility to avirulent *Pseudomonas syringae* but confer resistance to *Botrytis cinerea* in Arabidopsis. Plant Physiol 144: 1093–1103

Tang D, Wang G, Zhou JM (2017) Receptor kinases in plant-pathogen interactions: More than pattern recognition. Plant Cell 29: 618–637

Terras FRG, Torrekens S, Van Leuven F, Osborn RW, Vanderleyden J, Cammue BPA, Broekaert WF (1993) A new family of basic cysteine-rich plant antifungal proteins from Brassicaceae species. FEBS Lett 316: 233–240

Tsuji J, Jackson EP, Gage DA, Hammerschmidt R, Somerville SC (1992) Phytoalexin accumulation in *Arabidopsis thaliana* during the hypersensitive reaction to *Pseudomonas syringae* pv *syringae*. Plant Physiol 98: 1304–1309

Uemura T, Nakano RT, Takagi J, Wang Y, Kramer K, Finkemeier I, Nakagami H, Tsuda K, Ueda T, Schulze-Lefert P, et al (2019) A Golgi-released subpopulation of the Trans-Golgi network mediates protein secretion in Arabidopsis. Plant Physiol 179: 519–532

Vahisalu T, Kollist H, Wang Y-F, Nishimura N, Chan W-Y, Valerio G, Lamminmäki A, Brosché M, Moldau H, Desikan R, et al (2008) SLAC1 is required for plant guard cell S-type anion channel function in stomatal signalling. Nature 452: 487–491

van Loon LC, Rep M, Pieterse CMJ (2006) Significance of inducible defense-related proteins in infected plants. Annu Rev Phytopathol 44: 135–162

Wang L, Tsuda K, Sato M, Cohen JD, Katagiri F, Glazebrook J (2009) Arabidopsis CaM binding protein CBP60g contributes to MAMP-induced SA accumulation and is involved in disease resistance against *Pseudomonas syringae*. PLoS Pathog 5: e1000301

Williams CR, Baccarella A, Parrish JZ, Kim CC (2016) Trimming of sequence reads alters RNA-Seq gene expression estimates. BMC Bioinformatics 17: 103

Wu S, Shan L, He P (2014) Microbial signature-triggered plant defense responses and early signaling mechanisms. Plant Sci 228: 118–126

Xiao F, Goodwin SM, Xiao Y, Sun Z, Baker D, Tang X, Jenks MA, Zhou J-M (2004) Arabidopsis CYP86A2 represses *Pseudomonas syringae* type III genes and is required for cuticle development. EMBO J 23: 2903–2913

Xin X-F, He SY (2013) *Pseudomonas syringae* pv. tomato DC3000: A model pathogen for probing disease susceptibility and hormone signaling in plants. Annu Rev Phytopathol 51: 473–498

Xin XF, Nomura K, Aung K, Velásquez AC, Yao J, Boutrot F, Chang JH, Zipfel C, He SY (2016) Bacteria establish an aqueous living space in plants crucial for virulence. Nature 539: 524–529

Xu J, Meng J, Meng X, Zhao Y, Liu J, Sun T, Liu Y, Wang Q, Zhang S (2016) Pathogen-responsive MPK3 and MPK6 reprogram the biosynthesis of indole glucosinolates and their derivatives in Arabidopsis immunity. Plant Cell 28: 1144–1162

Yu G, Wang L-G, Han Y, He Q-Y (2012) clusterProfiler: An R package for comparing biological themes among gene clusters. OMICS 16: 284–287

Yu X, Feng B, He P, Shan L (2017) From chaos to harmony: Responses and signaling upon microbial pattern recognition. Annu Rev Phytopathol 55: 109–137

Yuan J, He SY (1996) The *Pseudomonas syringae* Hrp regulation and secretion system controls the production and secretion of multiple extracellular proteins. J Bacteriol 178: 6399–6402

Zhang N, Lariviere A, Tonsor SJ, Traw MB (2014) Constitutive camalexin production and environmental stress response variation in Arabidopsis populations from the Iberian Peninsula. Plant Sci 225: 77–85

Zhang Z, Wu Y, Gao M, Zhang J, Kong Q, Liu Y, Ba H, Zhou J, Zhang Y (2012) Disruption of PAMP-induced MAP kinase cascade by a Pseudomonas syringae effector activates plant immunity mediated by the NB-LRR protein SUMM2. Cell Host Microbe 11: 253–263

Zipfel C, Robatzek S, Navarro L, Oakeley EJ, Jones JDG, Felix G, Boller T (2004) Bacterial disease resistance in Arabidopsis through flagellin perception. Nature 428: 764–767